35th Annual International Conference of the IEEE EMBS
Osaka, Japan, 3 - 7 July, 2013

Simulation of a Current Source with a Cole-Cole Load for multi-frequency Electrical Impedance Tomography

Susana Aguiar Santos, Thomas Schlebusch and Steffen Leonhardt

***Abstract*— An accurate current source is one of the keys in the hardware of Electrical impedance Tomography systems. Limitations appear mainly at higher frequencies and for non-simple resistive loads. In this paper, we simulate an improved Howland current source with a Cole-Cole load. Simulations comparing two different op-amps (THS4021 and OPA843) were performed at 1 kHz to 1 MHz. Results show that the THS4021 performed better than the OPA843. The current source with THS4021 reaches an output impedance of 20 MΩ at 1 kHz and above 320 kΩ at 1 MHz, it provides a constant and stable output current up to 4 mA, in the complete range of frequencies, and for Cole-Cole (resistive and capacitive) load.**

***Index Terms*— Electrical Impedance Tomography (EIT), Improved Howland current source, Cole-Cole model**

I. INTRODUCTION

Electrical Impedance Tomography (EIT) is a non-invasive, non-harmful and low-cost imaging modality to map the impedance distribution of a body's section, by injecting small alternating currents and measuring the resulting voltages at the body [1], [2], [3]. In a multi-frequency EIT system, in order to create difference in frequency images, injection of current at different frequencies is necessary. Measuring more than one frequency at the same time, the measurement time is reduced [4]. There are two possible methods for multi-frequency injection: 1) the injection of one multi-sinus wave form and 2) the multiple injection of single sinus currents [5]. On the 1st case, just one current source is necessary, while in the 2nd multiple current sources perfect calibrated between them are necessary.

The precision of the injecting current has a great impact in the quality of reconstructed impedance images. A current source appropriated for an EIT system should have very high output impedance and a constant and steady current to the electrodes through all frequencies. It should be also load independent; being stable through both resistive and capacitive loads [2]. The research in current sources has been a frequent topic in hardware for EIT devices. Several research groups make use of Howland based current sources: the improved Howland [2], [6], [7], [8], [9], the modified Howland (DOA) [10], [11] and the Howland (with adjustable) GIC [2], [7], [10]. Non-Howland based current sources also appear, e.g., the CMOS Differential current source [12] or the current source ASIC [13].

As our interests are in multi-frequency EIT devices for medical applications, mainly focused on lung monitoring [3], the current source has to be able to inject a constant and steady current at least from 1 kHz to 1 MHz. For mfEIT applications, usually currents up to 5 mA are necessary for tissue characterization.

In this study, we adopted the improved Howland current source. We compare two different operation amplifiers, THS4021 and OPA843, for a Cole-Cole load.

S. Aguiar Santos, T. Schlebusch and S. Leonhardt are with the Philips Chair for Medical Information Technology, RWTH Aachen University, Aachen, Germany santos@hia.rwth-aachen.de

II. METHODOLOGY

A. The Improved Howland Current Source

The Howland current source is an op-amp based Voltage Controlled Current Source (VCCS), whose output is controlled by matching resistors of both positive and negative feedbacks. Howland based current sources are extensively used in EIT system because of its simplicity, feasible implementation, superior driving capability [9] and good performance when employed in single frequency injection [13]. Figure 1 shows the schematic of the improved Howland current source.

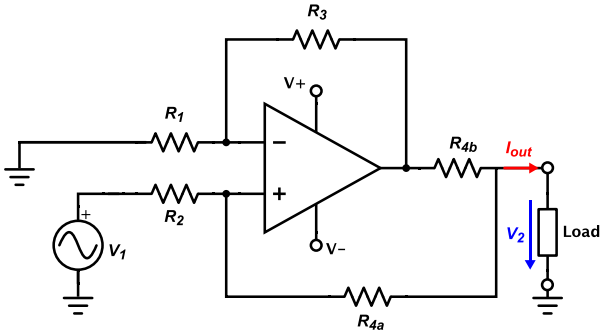

Fig. 1. Improved Howland current source circuit

The output current I_{out} is given by:

$$I_{out} = \frac{V_1}{R_i} - \frac{V_2}{R_o}, \tag{1}$$

where R_i is the input impedance and R_o the output impedance. The input and output impedances are defined by:

$$R_i = \frac{R_1 R_{4b}(R_2 + R_{4a})}{R_1(R_{4a} + R_{4b}) + R_{4a}R_3} \tag{2}$$

$$R_o = \frac{R_{4b}(1 + R_{4a}/R_2)}{(R_{4a} + R_{4b})/R_2 - (R_3/R_1)} \tag{3}$$

Theoretical, when both positive and negative feedbacks match the equation $(R_{4a} + R_{4b})/R_2 = R_3/R_1$, an infinite output impedance is reached. However, all resistors have

tolerances making the output impedance finite, depending of the drop voltage in the load and consequently being load dependent [8].

B. Cole-Cole Load

Our goal is to make a reliable and stable current source for EIT devices for medical purposes. Figure 2 shows how the current flows through the cells depending on the applied frequency. While at low frequencies the current flows around the cells, at higher frequencies the current penetrates the cell [14]. The electrical equivalent circuit for a biological tissue is represented by the Cole-Cole model on figure 3, where R_e represents the extracellular resistance, R_i is the intracellular resistance and C_m is the membrane capacitance. Thus, the Cole-Cole model was used as load in our study.

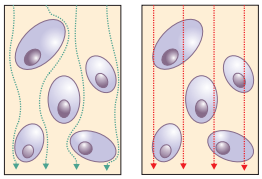

Fig. 2. Low and high-frequency current flow through the cells.

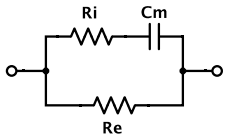

Fig. 3. Cole-Cole Model for biological objects. R_e is the extracellular resistance, R_i is the intracellular resistance and C_m is the membrane capacitance.

C. Operational Amplifiers

In Howland-based current sources, the amplifier must perform well at a wide frequency range higher than 1 MHz. Consequently, amplifiers were chosen mainly according with their speed characteristics. Two operational amplifiers by Texas Instruments were selected for this study: a 350-MHz bandwidth, low-noise, high-speed amplifier THS4021 and a wideband, low distortion, medium gain, voltage-feedback operational amplifier OPA843. On table I, some important parameters such has Bandwidth, Slew-Rate, Total Harmonic Distortion (THD) and Voltage supply (Vcc) of both amplifiers are presented.

TABLE I
COMPARISON OF THE SELECTED OPERATIONAL AMPLIFIERS

	THS4021	OPA843
Bandwidth (MHz)	350 MHz (G = 10)	260 MHz (G = 5)
Slew Rate (V/us)	470	1000
THD (Fc = 1 MHz) [dB]	-68	-95
Vcc (typ)	±5V to ±15V	±5V

III. RESULTS

The simulations of the improved Howland current source were performed using Cadence® Pspice® Lite 16.6 simulation tool. In the simulations, only one sweep parameter at each moment is possible to use. As in the current sources for EIT applications, the biggest problems are obtained with capacitive loads, in this paper we decided to present the results obtained for a Cole-Cole load with constant resistances and varying capacitance. The resistances were defined to $R_e = R_i = 2k\Omega$, and the capacitance varying for $C_m = 20, 40, 60, 80, 100pF$. Both amplifiers were supplied at $\pm 5V$, except on figure 6. Note that the curves for different C_m values are, in some graphics, overlapped, not being distinguishable due to the scale.

A. Output Current vs Time

The time-domain simulation results for both amplifiers at 50 kHz and 1 mA output current are presented on figure 4. For this case, both configurations present a precise and stable output current, apparently equal in both cases, for all C_m.

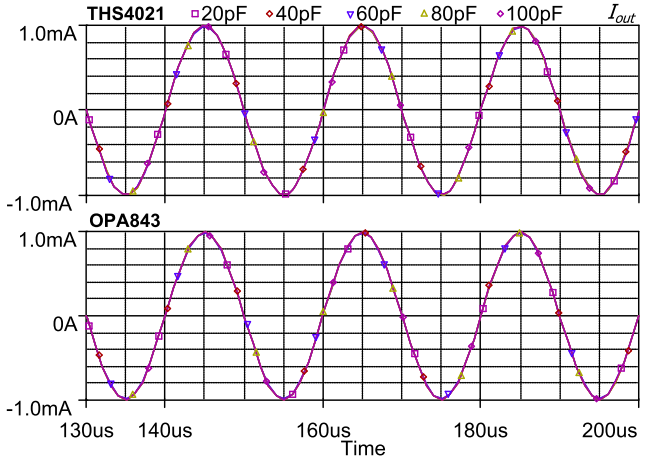

Fig. 4. Output current ($I_{out} = 1mA$) for both op-amps at 50 kHz, for a load with $R_e = R_i = 2k\Omega$, and varying $C_m = 20, 40, 60, 80, 100pF$

Figure 5 presents the results in the time-domain at 1 MHz and 1 mA output current. Also here both op-amps presented an equivalent result with precise and stable current output.

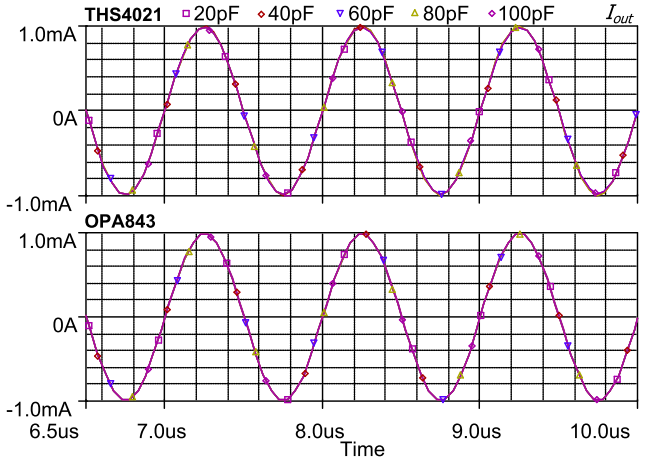

Fig. 5. Output current ($I_{out} = 1mA$) for both op-amps at 1 MHz, for a load with $R_e = R_i = 2k\Omega$, and varying $C_m = 20, 40, 60, 80, 100pF$

However, for medical applications, up to 5 mA currents are usually applied. In figure 6 the results at 1 MHz for an output current of 4 mA are presented. Here, with increase of the desired output current amplitude, the current output

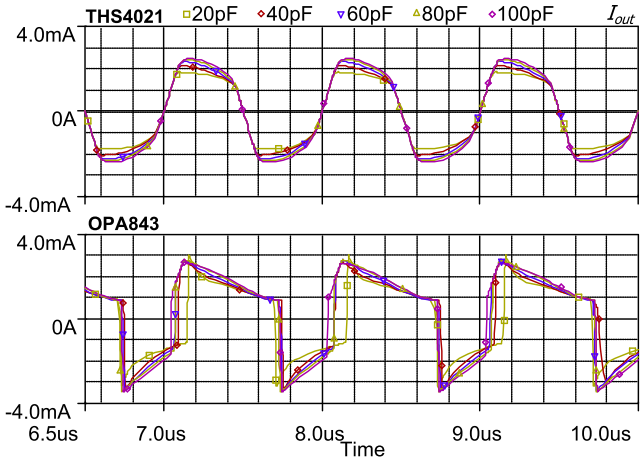

Fig. 6. Output current ($I_{out} = 4mA$) for both op-amps at 1 MHz, for a load with $R_e = R_i = 2k\Omega$, and varying $C_m = 20, 40, 60, 80, 100pF$, using a $V_{CC} = \pm 5V$

waveform gets significantly distorted, reaching less than 3 mA with both THS4021 and OPA843 amplifiers.

Nevertheless, the THS4021 op-amp, contrarily to the OPA843 that can be only supplied with ±5V, can be powered supplied with ±15V. Figure 7 presents the results for the THS4021 supplied at ±15V. A really stead output current is also achieved in this case, having an output current of 4 mA.

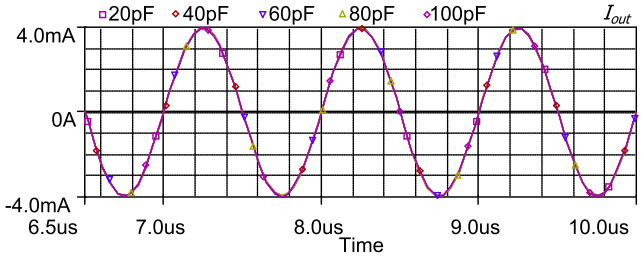

Fig. 7. Output current ($I_{out} = 4mA$) for THS4021 op-amp at 1 MHz, for a load with $R_e = R_i = 2k\Omega$, and varying $C_m = 20, 40, 60, 80, 100pF$, using a $V_{CC} = \pm 15V$

B. Output Current vs Frequency

In this chapter, frequency-domain analysis are performed. Figure 8 shows the current that flows through the R_e and the $R_i C_m$ parts of the load (fig. 3) for the THS4021 and OPA843 op-amps, respectively. As it was said in the methodology, at lower frequencies the current passes around the cells, i.e. in the extracellular compartment (R_e). At higher frequencies, the current penetrates the cell membrane (C_m) passing through the intracellular compartment (R_i), being visible the division of current in both parts. This behaviour is well observed in the results.

Nevertheless, figure 9 shows that the output current I_{out} (1 mA) of the current source maintains relative steady through all frequencies (1 kHz - 3 MHz), as it is desired, showing a good load-independence. Both plots are presented with the same scale in order to facilitate the interpretation. Additionally, table II presents the decrease in percentage (%) of the current output amplitude at 100 kHz and 1 MHz in comparison with 1 kHz, for both op-amps. Also here the THS4021 op-amp presented better results. While the output current using the THS4021 decreased only 0.09% - 0.13% of the I_{out} at 1 MHz, the output current using the OPA843 decreased between 0.33% - 0.48% at 1 MHz in comparison to 1 kHz.

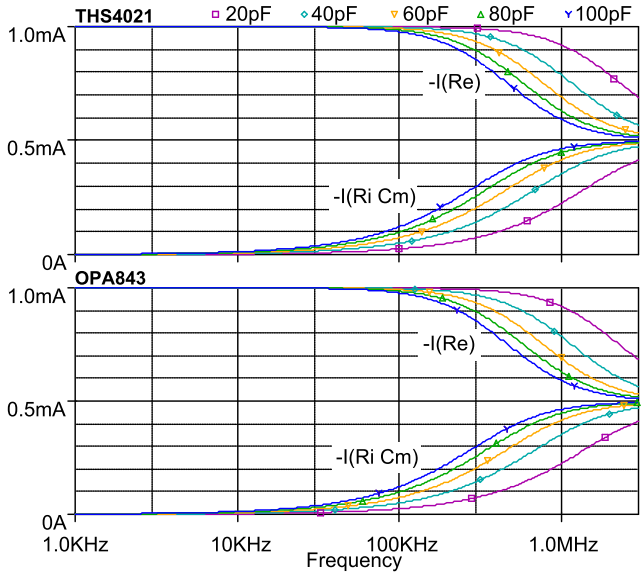

Fig. 8. Current flowing through the R_e and the R_i C_m parts of the load for both op-amps

TABLE II

DECREASE IN PERCENTAGE % OF THE OUTPUT CURRENT AMPLITUDE FOR 100 KHZ AND 1 MHZ, RELATIVELY TO 1 KHZ.

R_i=R_e=2kΩ	THS4021		OPA843	
C_m	100 kHz	1 MHz	100 kHz	1 MHz
20 pF	0.00	0.10	0.01	0.39
40 pF	0.00	0.13	0.01	0.48
60 pF	0.01	0.12	0.02	0.44
80 pF	0.01	0.10	0.02	0.38
100 pF	0.01	0.09	0.02	0.33

The Total Harmonic Distortion (THD) at 1 MHz (runtime = 100us, step = 0.05us) was 0.076% for the THS4021 and 0.0678% for the OPA843. Although the OPA843 present slightly better THD, the total amplitude decreasing of the output current at 1 MHz was higher, making the amplitude of the output current not so constant through the needed frequencies as with THS4021.

The Monte Carlo (MC) analysis performs the circuit response to the changes in the part values, varying randomly all parameters in the model for which a tolerance is specified. On figure 10, the MC analysis of the THS4021 for the worse capacitance performance tested (40 pF) is presented. Figure shows 50 runs for an uniform distribution of MC analysis. The current source resistors were defined with a tolerance of 0.1 %. The errors associated with the resistances tolerances are evident, being 1 mA output current just obtained with its perfect matching. However, for each run, the output current

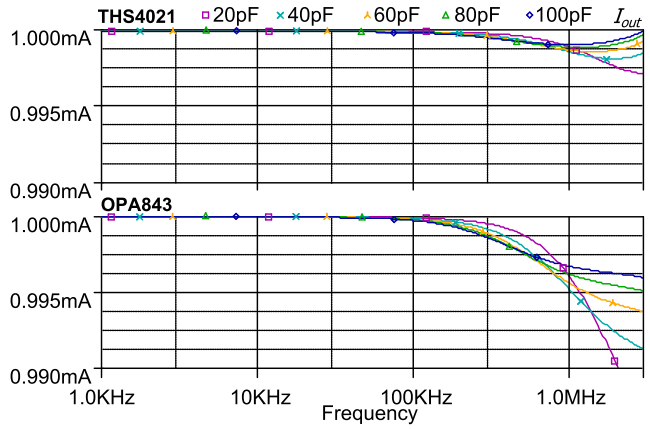

Fig. 9. Output current (I_{out}=1mA) for both op-amps, for a load with $R_e = R_i = 2k\Omega$, and varying $C_m = 20, 40, 60, 80, 100pF$

maintained relative constant through all frequencies up to 1 MHz (please pay attention to the scale). Through all 50 runs of the test, the decrease of the I_{out} was between 0.05% - 0.20 % at 1 MHz in comparison to 1 kHz.

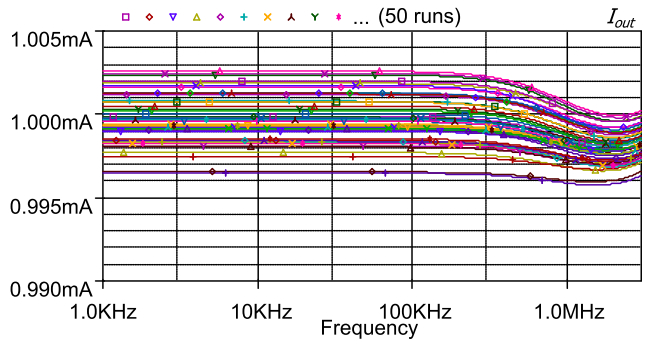

Fig. 10. Monte Carlo analysis of the output current ($I_{out} = 1mA$) for THS4021 op-amp. Load with $R_e = R_i = 2k\Omega$ and $C_m = 40pF$

C. Output Impedance

The output impedance (Z_{out}) of the current source for both op-amps is presented on fig. 11. Here the THS4021 amplifier presented also much higher Z_{out} in comparison with OPA843, reaching $20M\Omega$ at 1 kHz, $3M\Omega$ at 100 kHz and keeping above $320k\Omega$ at 1 MHz.

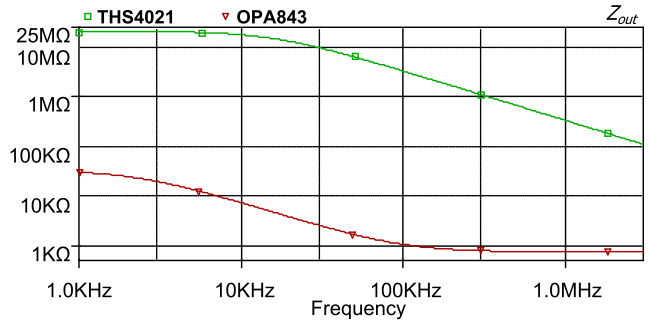

Fig. 11. Output impedance (Z_{out}) for both op-amps

Despite the good results, simulations generally tend to give much better results as in real measurements. This way, in the near future, an hardware test of this current source is planned.

IV. CONCLUSIONS

The results have shown that the improved Howland current source has a good performance using both THS4021 and OPA843 op-amps for output current as high as 1 mA, being the first one slightly better at 1 MHz. For higher current amplitudes, e.g., 4 mA, the THS4021 proved to be better, once by supplying the amplifier at $\pm$15V proved so good results as at 1 mA, which is not possible with the OPA843 due to its voltage supply limitation. The current source with THS4021 has shown high output impedance, good load independence, being able to supply up to 4 mA from 1 kHz to 1 MHz. This current source with THS4021 might be a good option for mfEIT systems. However, hardware measurements must be performed to correctly evaluate this current source.

ACKNOWLEDGMENT

Susana Aguiar Santos is supported by the PhD Grant SFRH/BD/76441/2011 awarded by the Portuguese Foundation for Science and Technology (FCT), Portugal.

REFERENCES

[1] J. Webster and P. Hughes, "Electrical impedance tomography," *Journal of Clinical Engineering*, vol. 16, no. 4, p. 349, 1991.

[2] W. Wang, M. Brien, D.-W. Gu, and J. Yang, "A comprehensive study on current source circuits," in *13th International Conference on Electrical Bioimpedance and the 8th Conference on Electrical Impedance Tomography*. IFMBE Proceedings, 2007, vol. 17, pp. 213–216.

[3] S. Leonhardt and B. Lachmann, "Electrical impedance tomography: the holy grail of ventilation and perfusion monitoring?" *Intensive Care Medicine*, vol. 38, no. 12, pp. 1917–1929, Sept. 2012.

[4] A. McEwan, G. Cusick, and D. S. Holder, "A review of errors in multi-frequency EIT instrumentation," *Physiological Measurement*, vol. 28, no. 7, pp. S197–S215, July 2007.

[5] H. Wi, P. Yoo, T. Oh, and E. Woo, "Cascaded multi-channel EIT system with fast data acquisition by frequency-division and space-division multiplexing," in *12th International Conference in Electrical Impedance Tomography (EIT 2011)*, 2011.

[6] D. Zhao, "High output-impedance current source for electrical impedance tomography." IEEE, Oct. 2011, pp. 1106–1109.

[7] A. S. Ross, G. J. Saulnier, J. C. Newell, and D. Isaacson, "Current source design for electrical impedance tomography," *Physiological Measurement*, vol. 24, no. 2, pp. 509–516, May 2003.

[8] J. W. Lee, T. I. Oh, S. M. Paek, J. S. Lee, and E. J. Woo, "Precision constant current source for electrical impedance tomography," in *Proceedings of the 25th Annual International Conference of the IEEE Engineering in Medicine and Biology Society, 2003*, vol. 2. IEEE, Sept. 2003, pp. 1066– 1069 Vol.2.

[9] Y. Wang, N. Li, H. Yu, Z. Sun, H. Nie, and H. Xu, "Study on wide-band voltage controlled current source for electrical impedance tomography." IEEE, Jan. 2012, pp. 1499–1502.

[10] Z. Li, Z. Xu, C. Ren, W. Wang, D. Zhao, and H. Zhang, "Study of voltage control current source in electrical impedance tomography system." IEEE, June 2010, pp. 1–4.

[11] T. K. Bera and N. Jampana, "A multifrequency constant current source suitable for electrical impedance tomography (EIT)." IEEE, Dec. 2010, pp. 278–283.

[12] J. Frounchi, M. H. Zarifi, and F. Dehkhoda, "A differential current source for high frequency biomedical applications in a 0.5 m CMOS integrated circuit technology," in *13th International Conference on Electrical Bioimpedance and the 8th Conference on Electrical Impedance Tomography*. IFMBE Proceedings, 2007, vol. 17, pp. 217–220.

[13] H. Hong, M. Rahal, A. Demosthenous, and R. H. Bayford, "Comparison of a new integrated current source with the modified howland circuit for EIT applications," *Physiological Measurement*, vol. 30, no. 10, pp. 999–1007, Oct. 2009.

[14] S. Grimnes and O. G. Martinsen, *Bioimpedance and bioelectricity basics*. London: Academic, 2008.